ISSN 0005–1144
ATKAAF 43(1–2), 69–74 (2002)

Nikša Burum, Zvonimir Šipuš

Radiation Properties of Spherical and Cylindrical Rectangular Microstrip Patch Antennas

UDK 621.396.67
IFAC IA 5.8.3

Original scientific paper

The program for calculating radiation properties of spherical and cylindrical rectangular microstrip patch antenna is presented. The patch can be embedded in or placed on a general multilayer spherical or circular-cylindrical structure. The solution procedure takes advantage of spectral-domain approach and the spherical/cylindrical multilayer structure is rigorously taken into account by calculating appropriate spectral-domain Green's functions. The results show the importance of rigorous analysis of curved patch antennas.

Key words: microstrip antennas, conformal antennas, moment methods, antenna array mutual coupling

1 INTRODUCTION

Microstrip patch antennas are often used because of their thin profile, light weight and low cost. Furthermore, they can be made to conform the structure. When the radius of the curved structure is large, the antenna can be analyzed as the planar one. However, for smaller radius of the structure more rigorous analysis methods should be used. If the antenna has a cylindrical shape, i.e. if one principal curvature is zero, the antenna can be analyzed as a circular-cylindrical one. In the case where both principal curvatures are different from zero the antenna can be analyzed as a spherical one.

The purpose of this paper is to describe the program for calculating radiation pattern of spherical and cylindrical rectangular microstrip patch antennas. Furthermore, the comparison of spherical and cylindrical patch antennas is given in order to show the importance of rigorous analysis of patch antennas on curved structures where both principal curvatures are different from zero.

2 METHOD OF ANALYSIS

The geometry of the problem is given in Figure 1. The rectangular patch is placed on or embedded in a multilayer spherical or cylindrical structure. The

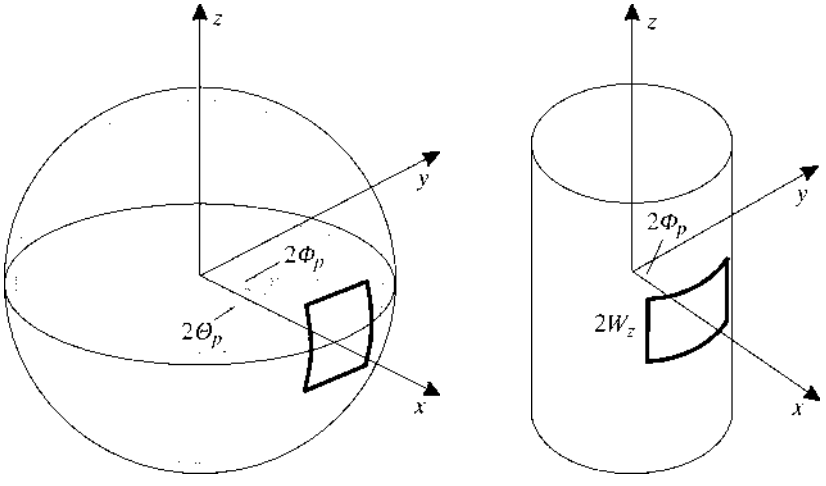

Fig. 1 Geometry of a conformal rectangular patch antenna; (a) patch antenna printed on a spherical structure, (b) patch antenna printed on a cylindrical structure

patch coordinates in the spherical coordinate system are $\pi/2-\theta_p \le \theta \le \pi/2+\theta_p$ and $-\phi_p \le \phi \le \phi_p$, and in the cylindrical coordinate system the are $-W_z \le z \le W_z$ and $-\phi_p \le \phi \le \phi_p$. The radiuses of the grounded sphere and the patch are a and b, respectively. We assume that the patch is resonant, i.e. the patch current is given by (for example, for spherical θ-polarized patch):

$$J_\theta(b,\theta,\phi) = \frac{1}{2\phi_p}\cos\left(\frac{\pi}{2\theta_p}\left(\theta-\frac{\pi}{2}\right)\right). \tag{1}$$

If we consider spherical, circular cylindrical and planar multilayer structures, they have one property in common: the structure is homogeneous in two dimensions, and varies in one dimension. For example, the spherical structure in Figure 1 varies in radial direction and it is homogeneous in θ and ϕ directions. Thus, we can call spherical, cylindrical and planar structures one-dimensional structures since they vary only in one dimension [1]. We simplify the problem of determining Green's functions for one-dimensional structures if we perform a two-dimensional Fourier transformation in the coordinates for which the structure is homogeneous [2, 3]. As a result, our original three-dimensional problem is transformed into a one-dimensional problem, which is much easier to solve. A drawback of this approach is that we usually have to solve the one-dimensional problem many times.

If we consider a problem defined in the cylindrical coordinate system we apply the Fourier transformation in axial direction, and Fourier series in ϕ-direction. For problems defined in the spherical coordinate system we apply the vector-Legendre transformation [4, 3]

$$\boldsymbol{J}(r,\theta,\phi) = \begin{bmatrix} J_r \\ J_\theta \\ J_\phi \end{bmatrix} = \sum_{m=-\infty}^{\infty}\sum_{n=|m|}^{\infty} \tilde{\boldsymbol{L}}(n,m,\theta)\,\tilde{\boldsymbol{J}}(r,n,m)\mathrm{e}^{jm\phi}, \tag{2a}$$

$$\tilde{\boldsymbol{J}}(r,n,m) = \\ = \frac{1}{2\pi S(n,m)}\int_{-\pi}^{\pi}\int_{0}^{\pi}\tilde{\boldsymbol{L}}(n,m,\theta)\boldsymbol{J}(r,\theta,\phi)\sin\theta\,\mathrm{e}^{-jm\phi}\mathrm{d}\theta\mathrm{d}\phi, \tag{2b}$$

$$\tilde{\boldsymbol{L}}(n,m,\theta) = \\ = \begin{bmatrix} P_n^{|m|}(\cos\theta)\sqrt{n(n+1)} & 0 & 0 \\ 0 & \dfrac{\partial P_n^{|m|}(\cos\theta)}{\partial\theta} & \dfrac{-jmP_n^{|m|}(\cos\theta)}{\sin\theta} \\ 0 & \dfrac{jmP_n^{|m|}(\cos\theta)}{\sin\theta} & \dfrac{\partial P_n^{|m|}(\cos\theta)}{\partial\theta} \end{bmatrix}, \tag{2c}$$

$$S(n,m) = \frac{2n(n+1)(n+|m|)!}{(2n+1)(n-|m|)!}. \tag{2d}$$

For θ-polarized spherical patch the patch current in the spectral domain is given by

$$\tilde{J}_\theta(b,n,m) = \frac{\sin(m\phi_p)}{m\phi_p}\frac{1}{2\pi S(n,m)}\cdot \\ \cdot\int_{\frac{\pi}{2}-\theta_p}^{\frac{\pi}{2}+\theta_p}\frac{\partial P_n^{|m|}(\cos\theta)}{\partial\theta}\cos\left(\frac{\pi}{2\theta_p}\left(\theta-\frac{\pi}{2}\right)\right)\sin\theta\,\mathrm{d}\theta, \tag{3a}$$

$$\tilde{J}_\phi(b,n,m) = \\ = \frac{j\sin(m\phi_p)}{\phi_p 2\pi S(n,m)}\int_{\frac{\pi}{2}-\theta_p}^{\frac{\pi}{2}+\theta_p}P_n^{|m|}(\cos\theta)\cos\left(\frac{\pi}{2_p\theta}\left(\theta-\frac{\pi}{2}\right)\right)\mathrm{d}\theta. \tag{3b}$$

Notice that there are both θ and ϕ current components in the spectral domain (in the spatial domain there is only θ component). This mixing of components when performing the Fourier transformation is preset only in spherical problems. Furthermore, notice that it is not possible to solve the integrals in (3a) and (3b) analytically, which is possible for circular-cylindrical and planar rectangular patches.

Planar, circular-cylindrical and spherical patch antennas are frequently analyzed by means of the electric field integral equation and the moment method. The kernel of the integral operator is a Green's function, which is different for different structures. There are two basic approaches for determining the Green's function of a general multilayer structure: either to analytically derive an expression for it and then to code this expression, or to develop a numerical routine for the complete calculation. The analytic approach requires less computer time than the numerical approach. However, it is a very laborious process to analytically determine the Green's functions for substrates with more than two layers. Therefore, in such cases it is convenient to use a numerical algorithm that determines the Green's function directly. Furthermore, the analytic approach requires often a new derivation of the Green's functions for a slightly different problem, such as for different number of layers or for different source locations inside the layers.

The G1DMULT algorithm [3] calculates the spectral-domain Green's functions in the same way for spherical, circular-cylindrical and planar geometries. The principle of the algorithm is as follows (e.g. for spherical geometry). For each value of spectral variables (n,m) the excited electromagnetic

field has the same variation in θ- and ϕ-directions as corresponding current component, i.e. only the field dependence in r-direction is unknown. The algorithm is based on dividing the multilayer problem into equivalent subproblems, one for each dielectric layer. The fields inside each layer are in the form (e.g. E_ϕ component)

$$\tilde{E}_\phi(r,n,m) = a^i_{nm}\hat{H}^{(2)}_n(k_i r) + b^i_{nm}\hat{J}_n(k_i r). \quad (4)$$

Here $\hat{H}^{(2)}_n$ and $\hat{J}_n$ are the Schelkunoff spherical Bessel and Hankel functions [5], k_i is the wave number in i^{th} layer, and a^i_{nm} and b^i_{nm} are the unknown coefficients to be determined. The equivalent subproblems are connected (and the coefficients a^i_{nm} and b^i_{nm} are calculated) by forcing the continuity of tangential components of electric and magnetic fields, i.e. we have four unknowns per boundary. The algorithm connects all equivalent subproblems into a system of $4\cdot(N_{\text{layer}}-1)$ linear equations with the same number of unknowns (N_{layer} denotes the number of layers). Once the amplitudes of the tangential fields have been determined, it is easy to determine the field amplitudes anywhere in the multilayer structure by applying the homogeneous region equivalent principle for the layer inside which we want to determine the field value. The core problem in the formulation is to calculate the E- and H- fields due to a harmonic current shell in a homogeneous region. The two subroutines that solve this subproblem (one for the electric source and one for the magnetic source) are the only part of the routine which depends on the geometry, and they are the only difference between three versions of the routine. More details about G1DMULT can be found in [3].

The far field radiation pattern is obtained as follows. If we consider e.g. the ϕ-component of the electric field in the outermost region with the r-coordinate larger than the r-coordinate of the patch, we have only outward-traveling waves described by

$$a^i_{nm}\hat{H}^{(2)}_n(k_0 r).$$

Therefore, in the outermost region we can connect the ϕ-component of the electric field with different r-coordinates r_1 and r_2 as

$$\tilde{E}_\phi(r_1,n,m) = \tilde{E}_\phi(r_2,n,m)\frac{\hat{H}^{(2)}_n(k_0 r_1)}{\hat{H}^{(2)}_n(k_0 r_2)} \approx$$

$$\approx \tilde{E}_\phi(r_2,n,m)\frac{j^{n+1}e^{-jk_0 r_1}}{\hat{H}^{(2)}_n(k_0 r_2)}. \quad (5)$$

Here r_1 represents the r-component of the far field pattern. The final solution is obtained by superposing the spectral solutions, see eq. (2a). In the similar way we calculate the radiation pattern of circular cylindrical patch antennas.

As an illustration of the near field radiation pattern, a mutual coupling coefficient of a two patch array is calculated. First step in determining S-parameters is to determine the currents on both patches, i.e. the integral equation for tangential components of the electric field is solved by applying the moment method. The entire-domain basis functions (see eq. (1)) and the Galerkin method are chosen inside the moment method. The elements of the moment method matrix Z_{ji} are calculated in the spectral domain

$$Z_{ji} =$$

$$= -\sum_{m=-\infty}^{\infty}\sum_{n=|m|}^{\infty} 2\pi S(n,m) r^2_{patch}\tilde{J}_j(-m,n)\tilde{G}(m,n)\tilde{J}_i(m,n). \quad (6)$$

Here $\tilde{G}$ is the spectral-domain Green function and J_i are the basis/test functions. If we have N patches in the array, then we need to solve the linear system $[Z][\alpha^k]=[V^k]$ N times ($k=1,...,N$), once for each excitation port. In more details, $[V^k]$ vectors correspond to a physical situation in which a unit current is entering the k^{th} port while the remaining $N-1$ ports are open-circuited. Fortunately, the matrix $[Z]$ is unchanged in all cases. After determining the amplitudes of basis functions $[\alpha^k]$ we calculate the voltage at port l by summation $-\sum_i V^l_i \alpha^k_i$ i.e., the lk element of the impedance port matrix is

$$Z^{\text{port}}_{lk} = -\sum_i V^l_i \alpha^k_i. \quad (7)$$

Scattering matrix elements are calculated from the impedance port matrix:

$$[S] = ([Z^{\text{port}}]-[Z^0])([Z^{\text{port}}]+[Z^0])^{-1} \quad (8)$$

where $[Z^0]$ is a diagonal matrix with elements Z^0 – the characteristic impedance of the feeding transmission lines.

3 NUMERICAL RESULTS

In this section the effects of the sphere size are illustrated. Furthermore, the comparison of radiation patterns of spherical, circular-cylindrical and planar patch antennas is given.

The quasi-square patch of dimension 4.8×4.8 cm is printed on the single-layer dielectric substrate with dielectric constant $\varepsilon_r = 2.38$ and thickness $h = 1.58$ mm. The working frequency is 2 GHz. The effect of the radius of the ground plane (grounded shell) is given in Figure 2. For comparison, the ra-

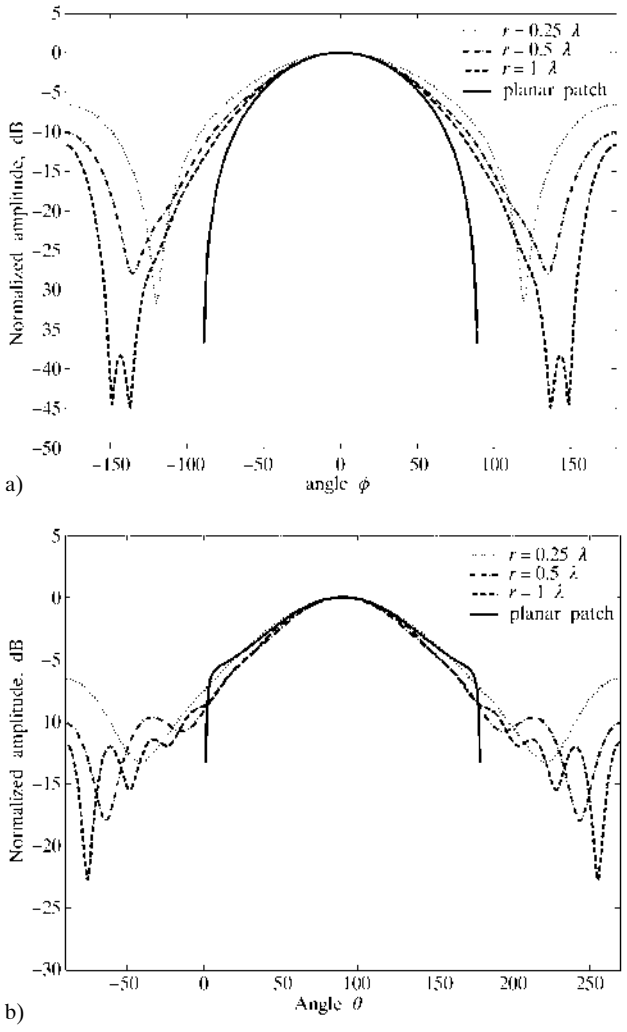

Fig. 2 Radiation pattern of a spherical rectangular patch antenna for different sphere radii; (a) H-plane, (b) E-plane

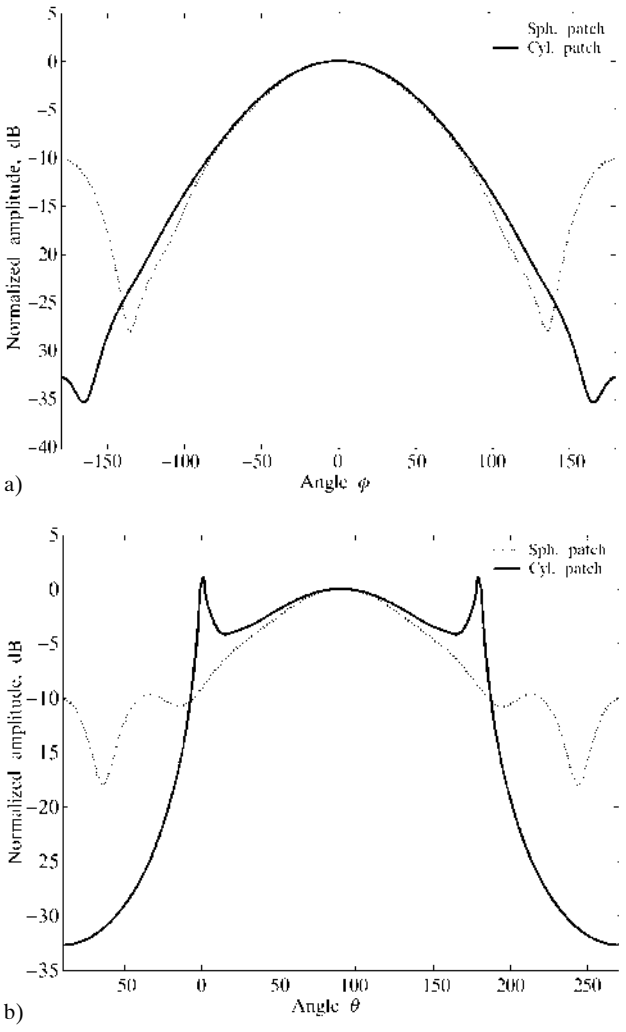

Fig. 3 Comparison between radiation patterns of spherical patch antenna and axially-polarized cylindrical patch antenna; (a) H-plane, (b) E-plane

diation pattern of planar patch antenna of same dimensions is also given. It can be seen that with enlarging the radius of the sphere the main lobe of the spherical patch antenna approaches the main lobe of the planar counterpart. As expected, the back-radiation is smaller for spheres with larger radius.

It is interesting to observe how well the curved patch with both principal curvatures different form zero can be approximated with a circular-cylindrical patch. In Figures 3 and 4 the comparison of radiation patterns of spherical and cylindrical patch antennas is given. Radius of the sphere and cylinder is $0.5\,\lambda_0$; other parameter values are the same as before. In Figure 3 the cylindrical patch is axially polarized, and in Figure 4 the cylindrical patch is ϕ-polarized. It can be seen that the cylindrical patch can be used as an approximation of the curved patch only in the azimuthal plane for both polarizations. In elevation plane the radiation pattern is significantly different, especially around the axis of the cylinder and in the back-side direction, which is due to the fact that the radiation pattern in the elevation plane »faces« the infinite structure of the cylinder.

The illustration of the near field radiation pattern is shown in Figure 5. The magnitude of the S_{21} parameter is shown as a function of spacing between patch centers. The radius of the sphere/cylinder is $1\,\lambda$, other dimensions are the same as in the previous example. The coupling between spherical patches in *E*- and *H*-plane is compared with cylindrical counterpart (both coupling in the axial direction ($y = 0$ plane in Figure 1.b) and in the ϕ-direction ($z = 0$ plane in Figure 1.b) are considered in

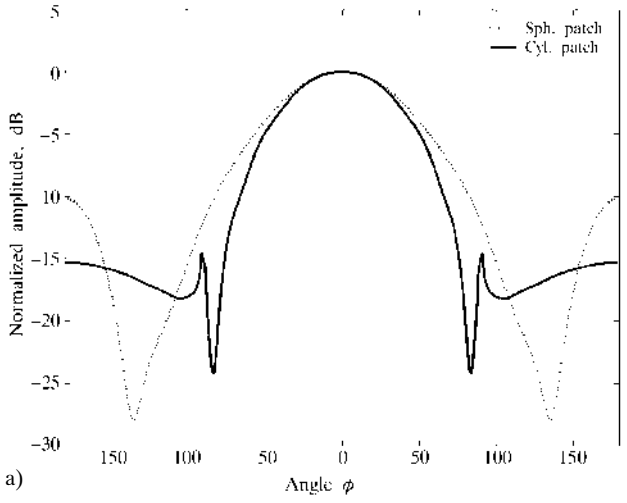

Fig. 4 Comparison between radiation patterns of spherical patch antenna and ϕ-polarized cylindrical patch antenna; (a) H-plane, (b) E-plane

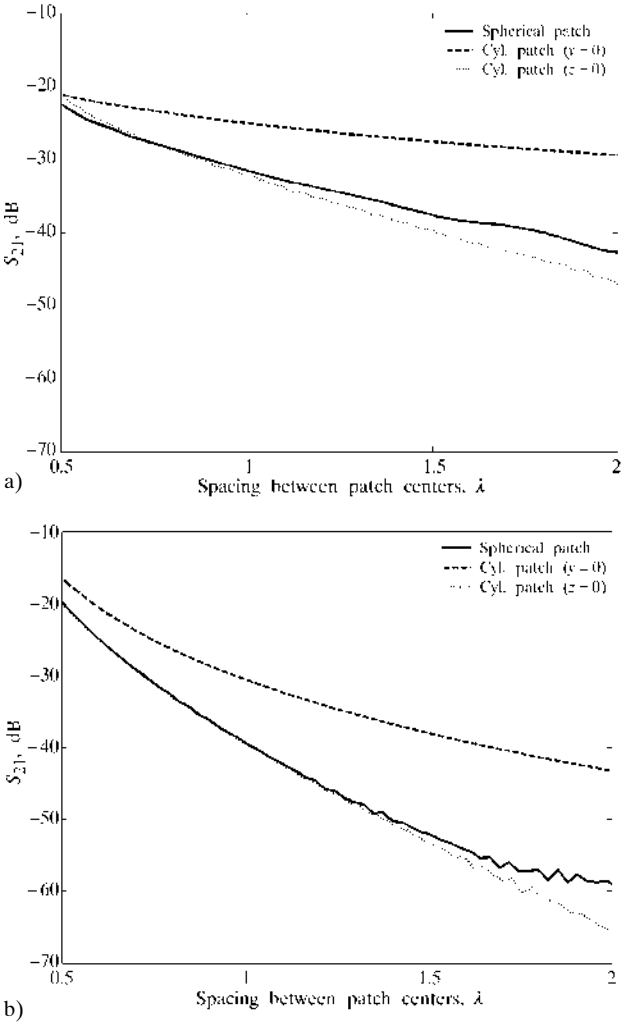

Fig. 5 Magnitude of S_{21} parameter shown as a function of spacing between patch centers; (a) E-plane, (b) H-plane

the cylindrical case). Again it can be seen that there is similarity between spherical and cylindrical cases only for coupling in the ϕ-direction. Notice that coupling in the axial direction is much stronger for cylindrical case than for the equivalent spherical case since the dielectric cylinder supports propagation of guided modes (surface waves) in the axial direction. Furthermore, notice that coupling in the *E*-plane is higher than in the *H*-plane since low-order surface waves has a maximum in the radiation pattern in the direction of the current flow (the radiation pattern of surface waves is considered along the dielectric interface).

4 CONCLUSION

The paper presents the program for calculating the near-field and the far-field radiation pattern of rectangular patch antenna printed on a spherical or circular-cylindrical structure. The problem is solved in spectral domain, i.e. for each value of spectral variables only onedimensional problem has to be solved. The general algorithm for calculating Green's functions is used in the program; therefore the patch can be printed on or embedded in a multilayer spherical or cylindrical structure. The program is tested by comparing the calculated radiation patterns of planar, circular-cylindrical and spherical patches.

Patch antennas on curved structures with both principle curvatures different from zero can be approximated with spherical or circular-cylindrical patches. If the radiation pattern in one plane only is of interest, both spherical and cylindrical approximations are suitable. However, circular-cylindrical

approximation is not appropriate for calculating the whole radiation pattern. Therefore, the program for analyzing spherical patch antennas is useful in analyzing patch antennas on general curved structures.

ACKNOWLEDGEMENT

This material is based upon work supported by the European Office of Aerospace Research and Development, Air Force Office of Scientific Research, Airforce Research Laboratory, under Contract No. F61775-01--WE024.

REFERENCES

[1] P.-S. Kildal, J. Sanford, **Analysis of Conformal Antennas by Using Spectral Domain Techniques for Curved Structures.** Proccedings of COST 245 – ESA workshop on active antennas, Noordwijk, The Netherlands, 1996, pp. 17–26.

[2] W. C. Chew, **Waves and Fields in Inhomogeneous Media.** IEEE Press, New York, 1995.

[3] Z. Sipus, P.-S. Kildal, R. Leijon, M. Johansson, **An Algorithm for Calculating Green's Functions for Planar, Circular Cylindrical and Spherical Multilayer Substrates.** Applied Computational Electromagnetics Society Journal, Vol. 13, No. 3., pp. 243–254, Nov. 1998.

[4] W. Y. Tam, K. M. Luk, **Resonances in Spherical-circular Microstrip Structures of Cylindrical-rectangular and Wrap-around Microstrip Antennas.** IEEE Trans. Microwave Theory Tech., Vol. 39, pp. 700–704, Apr. 1991.

[5] R. F. Harrington, **Time-harmonic Electromagnetic Fields.** McGraw-Hill, New York, 1961.

[6] Z. Sipus, P.-S. Kildal, **Analysis of Conformal Antennas on Multilayer Circular Cylindrical and Spherical Structures by Using G1DMULT**. Proceedings of AP2000 Millenium Conference on Antennas and Propagation, Davos, Switzerland, 2000, CD ROM.

[7] S. Raffaelli, Z. Sipus, P.-S. Kildal, **Analysis and Measurements of Arbitrarily Oriented Patches Mounted on Multilayer Circular Cylinder.** Submitted to IEEE Transaction on Antennas and Propagation.

Dijagram zračenja sfernih i cilindričnih mikrotrakastih antena pravokutnog oblika. U radu je predstavljen program za izračunavanje dijagrama zračenja sfernih i cilindričnih mikrotrakastih antena pravokutnog oblika. Mikrotrakasta antena može biti postavljena unutar ili na površinu općenite višeslojne sferne ili cilindrične strukture. U postupku rješavanja koriste se prednosti transformacije u spektralnu domenu pri čemu je sferna i cilindrična višeslojna struktura rigorozno uzeta u obzir uporabom odgovarajuće Greenove funkcije u spektralnoj domeni. Rezultati pokazuju važnost rigorozne analize zakrivljenih mikrotrakastih antena.

Ključne riječi: mikrotrakaste antene, konformne antene, metoda momenata, sprega između antenskih elemenata

AUTHORS' ADDRESSES:

Nikša Burum
Polytechnic of Dubrovnik
Ćira Carića 2, HR-20000 Dubrovnik, Croatia
fax: +385 20 445 743
e-mail: niksa.burum@vdu.hr

Zvonimir Šipuš
University of Zagreb
Faculty of Electrical Engineering and Computing
Unska 3, HR-10000 Zagreb, Croatia
e-mail: zvonimir.sipus@fer.hr

Received: 2002–10–05